AMERICAN JOURNAL OF PHYSIOLOGY
LUNG CELLULAR AND MOLECULAR PHYSIOLOGY

Am J Physiol Lung Cell Mol Physiol. 2009 Feb; 296(2): L176–L184. PMCID: PMC2643992
Published online 2008 Nov 14. doi: 10.1152/ajplung.90376.2008: 10.1152/ajplung.90376.2008 PMID: 19011050

Airway smooth muscle hyperplasia and hypertrophy correlate with glycogen synthase kinase-3β phosphorylation in a mouse model of asthma

J. Kelley Bentley,[1] Huan Deng,[1] Marisa J. Linn,[1] Jing Lei,[1] Gregoriy A. Dokshin,[1] Diane C. Fingar,[3] Khalil N. Bitar,[1] William R. Henderson, Jr.,[4] and Marc B. Hershenson[1,2]

The Departments of [1]Pediatrics and Communicable Diseases, [2]Molecular and Integrative Physiology, and [3]Cell and Developmental Biology, University of Michigan, Ann Arbor, Michigan; and [4]Department of Medicine, University of Washington, Seattle, Washington

Address for reprint requests and other correspondence: M. B. Hershenson, 1150 W. Medical Center Dr., Ann Arbor, MI 48109-0688 (e-mail: mhershen@umich.edu)

Received 2008 Jul 8; Accepted 2008 Nov 10.

Abstract

Increased airway smooth muscle (ASM) mass, a characteristic finding in asthma, may be caused by hyperplasia or hypertrophy. Cell growth requires increased translation of contractile apparatus mRNA, which is controlled, in part, by glycogen synthase kinase (GSK)-3β, a constitutively active kinase that inhibits eukaryotic initiation factor-2 activity and binding of methionyl tRNA to the ribosome. Phosphorylation of GSK-3β inactivates it, enhancing translation. We sought to quantify the contributions of hyperplasia and hypertrophy to increased ASM mass in ovalbumin (OVA)-sensitized and -challenged BALB/c mice and the role of GSK-3β in this process. Immunofluorescent probes, confocal microscopy, and stereological methods were used to analyze the number and volume of cells expressing α-smooth muscle actin and phospho-Ser^{9} GSK-3β (pGSK). OVA treatment caused a 3-fold increase in ASM fractional unit volume or volume density (Vv) (PBS, 0.006 ± 0.0003; OVA, 0.014 ± 0.001), a 1.5-fold increase in ASM number per unit volume (Nv), and a 59% increase in volume per cell (Vv/Nv) (PBS, 824 ± 76 μm^3; OVA, 1,310 ± 183 μm^3). In OVA-treated mice, there was a 12-fold increase in the Vv of pGSK (+) ASM, a 5-fold increase in the Nv of pGSK (+) ASM, and a 1.6-fold increase in Vv/Nv. Lung homogenates from OVA-treated mice showed increased GSK-3β phosphorylation and lower GSK-3β activity. Both hyperplasia and hypertrophy are responsible for increased ASM mass in OVA-treated mice. Phosphorylation and inactivation of GSK-3β are associated with ASM hypertrophy, suggesting that this kinase may play a role in asthmatic airway remodeling.

Keywords: ovalbumin, remodeling, stereology

INCREASED AIRWAY SMOOTH MUSCLE (ASM) mass is a characteristic finding in fatal and nonfatal asthma. Increased ASM mass may be caused by hyperplasia (an increase in cell number) or hypertrophy (an increase in cell size). Few studies have addressed the cellular mechanism of increased ASM mass in asthma. Ebina and colleagues (9) distinguished two asthmatic subtypes, one in which smooth muscle hyperplasia was present only in the central bronchi and another in which ASM hypertrophy was present throughout the airway tree. Benayoun and colleagues (5) found that the airways of patients with severe asthma had larger smooth muscle cell diameter and increased expression of α-smooth muscle actin and myosin light-chain kinase, further evidence that smooth muscle hypertrophy contributes to airway remodeling in asthma. Finally, Woodruff and colleagues (39) found that ASM cell number was nearly twofold higher in subjects with mild-to-moderate asthma, whereas there was no increase in cell size between groups. Also, although α-smooth muscle actin immunoreactivity increased by 50–83%, the mRNA expression of contractile protein genes was not increased, consistent with the notion that α-smooth muscle actin expression may be regulated in a posttranscriptional manner. These reports are consistent with clinical studies suggesting the existence of different asthma phenotypes (38).

To obtain additional mechanistic information regarding mechanisms of ASM remodeling, we studied mice undergoing ovalbumin (OVA) sensitization followed by repeated challenge. This model has been previously demonstrated to induce features of airway remodeling including thickening of the peribronchial smooth muscle layer (15, 16, 18, 19, 24, 26, 32, 35).

Hypertrophic growth, if present, may occur via increased transcription of contractile apparatus proteins, increased translation of contractile apparatus mRNA, or reduced proteolysis. Protein synthesis is controlled, in part, through the action of glycogen synthase kinase (GSK)-3β, a constitutively active kinase that inhibits eukaryotic initiation factor (eIF)-2 activity, thereby limiting binding of methionyl tRNA to the 40S ribosomal subunit. However, Ser^{9} phosphorylation of GSK-3β by the serine/threonine kinase Akt inactivates it, leading to a general enhancement of translation initiation. GSK-3β also negatively regulates transcription factors involved in muscle-specific gene expression, including nuclear factors of activated T cells (NFAT), GATA4, and β-catenin (1, 2, 12, 13, 21, 30, 36). We (7) have shown in cultured ASM cells that inhibition of GSK-3β induces hypertrophy via two mechanisms. First, GSK-3β inhibition increased protein synthesis and contractile protein expression via eIF2B-dependent translation. Second, inhibition of GSK-3β increased the transcription of α-smooth muscle actin via transactivation of NFAT and serum response factor.

We hypothesized that both hyperplasia and hypertrophy contribute to increased ASM mass in OVA-sensitized and -challenged mice and that GSK-3β plays a role in this process. We show for the first time that both hyperplasia and hypertrophy are responsible for increased ASM mass in OVAtreated mice. Furthermore, phosphorylation and inactivation of GSK-3β is associated with ASM hypertrophy, suggesting that this kinase may play an important role in asthmatic airway remodeling.

METHODS

Cell culture of mouse ASM cells. All animal use was done in accordance with National Institutes of Health (NIH) and university guidelines as administered by the University Committee on Use and Care of Animals at the University of Michigan, which approved this study. Cells were prepared from lungs by collagenase digestion of minced dissected airways followed by migration from explants as previously described (7). Cultures were serum-deprived and treated with transforming growth factor (TGF)-β (10 ng/ml) or the GSK-3β inhibitors LiCl (10 mM), SB-216763 (50 nM) or 4-benzyl-2-methyl-1,2,4-thiadiazolidine-3,5-dione (TDZD)-8 (9 μM).

Immunoblotting. Mouse ASM cells or lung tissues were washed briefly in cold PBS and homogenized in a buffer containing 50 mM Tris (pH 7.5), 100 mM NaCl, 50 mM NaF, 40 mM β-glycerophosphate, 2 mM EDTA, 200 μM Na_3VO_4, and 1% Triton X-100 containing complete protease inhibitors (Roche Diagnostics, Indianapolis, IN) for 30 s with a handheld rotor-stator-type tissue homogenizer (model 98530-395; Biospec Products, Bartlesville, OK) and centrifuged a 10,000 *g* for 30 min to remove nuclei and cell particles. Supernatants were resolved by SDS-PAGE and transferred to nitrocellulose. Membranes were probed with mouse anti-α-smooth muscle actin (MAb 1A4; Calbiochem, San Diego, CA), mouse anti-myosin heavy chain (MHC) (MAb HSM-V; Sigma-Aldrich, St. Louis, MO), rabbit anti-phospho-Ser^9 GSK-3β (pGSK), or rabbit anti-total GSK-3β (both from Cell Signaling Technology, Danvers, MA). When needed to visualize α-smooth muscle actin immunoreactivity, a horseradish peroxidase conjugate of rat anti-mouse κ-light chain was used.

Flow cytometry. Flow cytometry was performed to determine cell size (by forward scatter) and α-actin expression. Cells were removed from the plates by trypsin, washed with Ca^{2+}- and Mg^{2+}-containing PBS, and fixed with 50% ethanol for 20 min at −20°C. The ethanol was removed by PBS washes, and cells were blocked with 1% BSA in PBS for 20 min at 4°C. Cells were stained with 2.5 μg/ml FITC-conjugated anti-α-actin (30 min at 4°C; Sigma-Aldrich). Cells were finally washed with PBS and processed on a FACSCalibur flow cytometer (BD Biosciences, San Diego, CA).

Fluorescence microscopy of cultured cells. Mouse ASM cells were grown on collagen-coated glass slides (BD Biosciences) and fixed in 1% paraformaldehyde. For immunofluorescence, slides were probed with phospho-GSK-3β antibody or anti-NFATc3 (Santa Cruz Biotechnology, Santa Cruz, CA) followed by Alexa 488-labeled goat anti-rabbit IgG (Molecular Probes, Eugene, OR) and Cy3-conjugated mouse anti-α-smooth muscle actin-Cy3 (Sigma-Aldrich). Nuclei were visualized with Hoechst 33342 (Sigma-Aldrich). Cells were imaged using a Zeiss LSM 150 confocal microscope (Carl Zeiss, Thornwood, NY).

OVA sensitization and challenge. Mice (BALB/c; Charles River Laboratories, Wilmington, MA) were sensitized to sterile LPS-free OVA (Pierce, Rockford, IL) or PBS control by intraperitoneal injection and serially challenged over a month with intranasal instillations of OVA or PBS (Fig. 1*A*) in a modification of protocols previously described (16, 18).

Measurement of airways responsiveness. Changes in airway dynamic resistance in response to increasing doses of nebulized methacholine were measured using a forced oscillation technique (flexiVent; SCIREQ, Montréal, Québec, Canada). All mice were anesthetized with sodium pentobar-

bital (6.5 mg/kg mouse) and intubated via cannulation of the trachea with a 20-gauge stub adapter cannula (Becton Dickinson, Sparks, MD). Mechanical ventilation was performed at 150 breaths/min with a tidal volume of 10 ml/kg body wt.

Immunohistochemical staining of mouse lung sections for α-smooth muscle actin. Selected sections were blocked with a mouse-on-mouse blocking kit (Vector Laboratories, Burlingame, CA) and immunostained for α-smooth muscle actin or background using 1 μg/ml MAb 1A4 or its mouse IgG_{2a} isotype control (BD Biosciences). Color was developed using the peroxidase reaction with diaminobenzidine and $NiCl_2$ enhancement.

Tissue preparation for fluorescence confocal microscopy. The pulmonary artery was perfused with EDTA. Mouse lung vasculature was perfused with 5 mM EDTA in PBS injected through the pulmonary artery until the lung blanched. Lungs were inflated to 30 cmH_2O pressure with 4% paraformaldehyde (Sigma-Aldrich) and placed in formalin overnight. Both lungs were placed in cassettes in a random orientation to allow the systematic uniform random sampling required for stereological morphometry (8, 23). From a random start, paraffin-embedded lungs were sectioned every 250 μm, alternating between 5- and 50-μm-thick sections. The number of section pairs varied from between 8 and 17, depending on the length and orientation of the lungs. Slides were probed with phospho-GSK-3β antibody (Cell Signaling Technology) followed by Alexa 488-labeled goat anti-rabbit IgG and Cy3-conjugated mouse anti-α-smooth muscle actin (clone 1A4; Sigma-Aldrich). Nuclei were visualized with Hoechst 33342 (Sigma-Aldrich).

Stereological morphometry of mouse ASM cell volume and number. Initially, we randomly superimposed low power (×1.25) images of each section with a 0.104-cm^2 grid (NIH ImageJ; NIH, Bethesda, MD) to determine total sectional area by the Cavalieri point-counting method (8, 23). The Cavalieri lung volume, Vref, was calculated as the sum of the points lying on each individual lung section × the area per point × the distance between the sections. Sixty-two slides from 6 PBS-treated animals and 80 slides from 6 OVA-treated animals were examined. Immunofluorescent probes and stereological methods were then combined with confocal microscopy to analyze the number and volume of cells expressing the contractile protein α-smooth muscle actin and pGSK. For each experimental section, a rabbit IgG and mouse IgG control section at the same concentrations (1 μg/ml) was examined to set the confocal background staining to 0.

To quantify the volume of ASM, one randomly chosen field of each 5-μm-thick tissue section was photographed at ×100. A crossgrid (NIH ImageJ) was superimposed on each image, and both the total number of points and the number of points falling on α-actin (+) ASM were counted. Only ASM in structures larger than alveolar ducts were counted. The identical procedure was followed for pGSK. Volume density, Vv, was calculated as the sum of the points in the reference space divided by the total number of points counted. Vv was multiplied by lung volume, as obtained by the total water displacement method, to calculate total ASM volume. For the PBS-treated group, the coefficient of variation was 0.184, and the sampling error was 0.023. For the OVA-treated group, the coefficient of variation was 0.443, and the sampling error was 0.049.

For nuclear counts, 1 random field of each 50-μm-thick tissue section was photographed at ×400, and a *z*-series stack of 20 individual 1.5-μm sections was obtained using a Zeiss confocal microscope with a 5-μm guard distance from the cut surface of each section. This allowed sequential counts of ASM nuclei as they came into focus (27). To quantify nuclei, a randomized uniform 23.252-μm^2 grid was overlaid on each image in the stack using NIH ImageJ in which 16 nonadjacent squares were used to establish 16 columns for nuclear counting using the optical disector. Nuclear density (Nv) was calculated as the sum of the objects counted/(number of disectors × volume of 1 dissector). Total lung nuclear number was determined using the Cavalieri reference volume to avoid shrinkage artifacts. From this, the total lung nuclear number, N, was calculated by the formula Nv × Vref. Nuclei in pGSK-positive cells were only counted if the cells were α-actin-positive.

In vitro GSK-3β kinase assay. GSK-3β activity was measured by immunoprecipitating lung homogenates with mouse anti-GSK-3β (clone GSK-4B; Sigma-Aldrich) and incubating immunoprecipitates with the GSK-3β substrate tau (1 μg/μl; Sigma-Aldrich), ATP (1 mM), and [γ-^{32}P]ATP (10 μCi) for 30 min at 30°C as previously described (34). Reaction mixtures were subjected to SDS-PAGE, transferred to nitrocellulose, and exposed to film. Total GSK-3β in the immunoprecipitates was examined using rabbit anti-GSK-3β.

RESULTS

TGF-β and GSK-3β inhibitors increase mouse ASM cell size and α-smooth muscle actin synthesis. Previous work from our laboratory (7) has shown that TGF-β and chemical inhibitors of GSK-3β increase human ASM cell size and α-actin synthesis. We also showed that mouse ASM cells isolated from OVA-treated mice demonstrate increased cell size and α-actin expression. We examined the effect of TGF-β and GSK-3β inhibitors on cultured mouse ASM cells. As in human cells, mouse cells demonstrated increased α-smooth muscle actin expression and pGSK content in response to treatment with either 10 ng/ml TGF-β, 10 mM LiCl, or 50 nM SB-216763 (Fig. 1, *A* and *B*), whereas TGF-β and both GSK-3β inhibitors significantly increased protein abundance of α-actin and MHC. pGSK was increased by TGF-β and LiCl treatment (SB-216763 is a competitive inhibitor of GSK-3β and would not be expected to consistently increase GSK-3β phosphorylation). TGF-β and both GSK-3β inhibitors increased cell size and α-actin content as assessed by flow cytometry (Fig. 1*C*). Finally, TGF-β, LiCl, and SB-216763 each increased levels of pGSK and NFATc3 in both the cytoplasm and cell nucleus (Fig. 1*D*). Together with our previous work (7), these data suggest that GSK-3β phosphorylation and inactivation may play a role in allergic airway inflammation and remodeling.

OVA sensitization and challenge increases airway inflammation and smooth muscle deposition. As observed by other investigators, OVA sensitization and challenge induced increased reactivity to inhaled methacholine (Fig. 2). In lungs from OVA-treated mice, sensitization was accompanied by an increase in airway inflammation as demonstrated by monocytic and eosinophilic infiltration of the airways (Fig. 3, *inset*). At the same time, smooth muscle accumulation around the airways was increased, as detected by hematoxylin and eosin staining and verified by increased α-smooth muscle actin immunohistochemistry (Fig. 3). Immunofluorescence allowed clearer visualization of nuclei and α-actin immunostaining.

Increased α-actin expression is quantitatively associated with increased ASM volume. The Cavalieri point-counting method was used to determine total ASM volume. The contractile protein α-smooth muscle actin was used as a marker for ASM. Immunofluorescent images from random portions of lung tissue were examined. OVA sensitization and challenge significantly increased the Vv of α-smooth muscle actin around the airways, from an average of 0.006 to 0.014 (Table 1). OVA treatment also increased total ASM volume per lung over threefold from a mean of 0.005 to 0.017 ml.

Increases in ASM volume could result from hyperplasia, hypertrophy, or a combination of these 2 mechanisms. To determine whether the increase in ASM tissue volume was accompanied by an increase in cell number, as well as to gain an estimate of individual cell size, a 2-stage stereological method using the optical dissector and Cavalieri estimator was used. Average ASM Nv increased 1.5-fold, from 7.09×10^6 to 10.9×10^6 (Table 1). The total number of ASM cells per lung increased 2-fold from 6.03×10^6 to 12.8×10^6. The average volume of α-actin expressing ASM cell (Vv/Nv) was increased 1.6-fold by OVA sensitization, from 824 to 1,310 μm^3.

OVA sensitization and challenge increases lung pGSK immunofluorescence. Protein synthesis is controlled, in part, through the action of GSK-3β, a constitutively active kinase that inhibits eIF2 activity, thereby limiting binding of methionyl tRNA to the 40S ribosomal subunit. Ser^9 phosphorylation of GSK-3β by the serine/threonine kinase Akt inactivates it, leading to a general enhancement of translation initiation. GSK-3β also negatively regulates transcription factors involved in ASM contractile apparatus gene expression (7). We found that pGSK immunoreactivity was increased in the OVA-treated mice (Figs. 4 and 5). Sections revealed a generalized increase in pGSK immunoreactivity in the respiratory epithelium, vascular smooth muscle, ASM, and inflammatory tissues. In the large and mid-sized airways, fluorescence microscopy demonstrated colocalization of α-smooth muscle actin and pGSK. There was a 12-fold increase in ASM pGSK Vv, from 0.001 to 0.012 (Table 2). OVA treatment increased total ASM pGSK volume per lung from 0.001 to 0.015 ml per lung. The Vv of ASM that did not immunostain for pGSK was statistically the same for PBS and OVA-treated mice. The ASM cell number associated with pGSK also increased in lungs from the treated mice. There was a 5-fold increase in the Nv of ASM cells with pGSK, with a 7-fold increase in the absolute number of pGSK-expressing cells per lung. The cell size of pGSK-positive ASM cells also increased. The average size of ASM cells with immunodetectable pGSK increased from 768 μm^3 with PBS treatment to 1,230 μm^3 with OVA treatment, a 1.6-fold increase. The average size of cells without pGSK did not change with OVA treatment (PBS, 802 μm^3; OVA, 722 μm^3).

OVA sensitization and challenge whole lung GSK-3β phosphorylation and activity. Lung homogenates were obtained from control and OVA-treated mice. Homogenates from OVA-treated mice expressed greater amounts of α-smooth muscle actin but not β-actin (Fig. 6). Homogenates from treated mice also demonstrated greater levels of pGSK but not total GSK-3β. Lung GSK-3β activity was assessed by immunoprecipitating homogenates with anti-GSK-3β and performing an in vitro kinase assay using tau protein as a substrate. OVA sensitization and challenge lowered whole lung GSK-3β activity.

DISCUSSION

Few studies have addressed the cellular mechanism of increased ASM mass in asthma (5, 9, 39). Given the paucity of clinical data examining this question, we studied mice undergoing OVA sensitization followed by repeated challenge, a model that has been previously demonstrated to induce features of airway remodeling in mice and rats, including thickening of the peribronchial smooth muscle layer (15, 16, 18, 19, 24, 26, 32, 35). ASM mass increased, in part, by cellular proliferation, as evidenced by bromodeoxyuridine uptake (26, 32), proliferating cell nuclear antigen immunostaining (19, 35), and cell number per millimeter of basement membrane (24). However, no studies have systematically examined ASM cell number and size using advanced stereological techniques. Consistent with previous studies, we found that OVA sensitization and challenge of BALB/c mice caused a 3-fold increase in the ASM Vv, a measure of ASM mass, as well as a 1.5-fold increase in ASM Nv, a measure of smooth muscle cell number. Furthermore, we found that OVA treatment induced a 59% increase in Vv/Nv, a measure of cell volume. Average volume per cell increased from 824 to 1,310 μm^3. Together, these data demonstrate that allergen sensitization and challenge induces ASM hypertrophy as well as hyperplasia and are consistent with human studies showing ASM hypertrophy in human asthma (5, 9).

ASM cells were identified by expression of α-smooth muscle actin. OVA treatment increased ASM Vv as well as the total ASM volume per lung. ASM cells isolated from OVA-treated mice showed greater α-smooth muscle immunocytochemical staining. Although we did not examine the expression of other muscle proteins, these data suggest that allergic sensitization and challenge increases ASM contractile protein expression. These data contrast with data from Moir and colleagues (20), who found that OVA-sensitized and -challenged Brown Norway rats paradoxically decreased small bronchiole expression of smooth muscle MHC isoform 1, calponin, smoothelin-A, and myosin light-chain kinase. This discrepancy could be due to differences in species, airway size, and contractile protein of interest.

Having confirmed our hypothesis that both hypertrophy and hyperplasia contribute to ASM remodeling in allergen-treated mice, we sought to examine the potential role of GSK-3β in this process. GSK-3β is a serine/threonine kinase that is constitutively active and becomes inactivated on phosphorylation at Ser^9 (6). The serine/threonine kinase Akt is the major GSK-3β kinase. Accumulated evidence suggests that GSK-3β negatively regulates cardiac (1, 3, 12, 22), skeletal muscle (31, 36), and ASM hypertrophy (7). GSK-3β negatively regulates transcription factors involved in muscle-specific gene expression, including NFAT, GATA4, and β-catenin and serum response factor (1, 2, 12, 13, 21, 30, 36). Our new data show that GSK-3β inhibition with SB-216763 increases nuclear localization of NFAT. GSK-3β also positively regulates p65 RelA binding to a subset of NF-κB-regulated genes, including those for interleukin-6 and monocyte chemoattractant protein-1 (33). Finally, phosphorylation of the GTPase-activating protein tuberous sclerosis complex (TSC)-2 by GSK-3β increases the ability of TSC-2 to inhibit mammalian target of rapamycin (mTOR) signaling (17). Other downstream targets of GSK-3β regulate muscle hypertrophy via the translational process. One of the critical steps controlling the initiation of protein translation is formation of the 43S preinitiation complex. eIF2, a multimer consisting of α-, β-, and γ-subunits, functions to recruit methionyl tRNA and conduct it as a tRNA-eIF2-GTP ternary complex to the 40S ribosomal subunit. eIF2 GTP loading is determined by the activity of eIF2B, a guanine nucleotide ex-

change factor. eIF2Bε Ser^{539} phosphorylation by GSK-3β inhibits its GDP/GTP exchange activity, thereby limiting binding of methionyl tRNA to the 40S ribosomal subunit. However, phosphorylation of GSK-3β by Akt inactivates it, leading to eIF2B dephosphorylation and activation and a general enhancement of translation initiation (14, 37).

Since mRNA translation and protein synthesis is required for both cell proliferation and hypertrophy, we hypothesized that phosphorylation of GSK-3β contributes to ASM remodeling. Previous studies have demonstrated a role for GSK-3β in the proliferation of cultured human ASM cells (11, 25). We found that pGSK immunoreactivity was increased in the OVA-treated mice and that α-smooth muscle actin and pGSK colocalized in the large and mid-sized airways. OVA treatment increased ASM pGSK Nv and the total number of cells per lung. Furthermore, the cell size of pGSK-positive ASM cells increased from 768 μm^3 with PBS treatment to 1,230 μm^3 with OVA treatment. The average size of cells without pGSK did not change. Finally, bronchial smooth muscle cells isolated from OVA-treated mice were larger and showed greater levels of pGSK and GSK-3β kinase activity. Since phosphorylation and inactivation of GSK-3β is associated with ASM hypertrophy, these data suggest that GSK-3β plays an important role in asthmatic ASM remodeling.

It has recently been shown that intravenous administration of the chemical GSK-3β inhibitor TDZD-8 1 h before OVA challenge decreases airways inflammation, mucus production, and hyperresponsiveness in BALB/c mice (4). Western blot analysis of whole lung lysates and normal human epithelial cells revealed decreased phosphorylation of p65 RelA. This study suggests that GSK-3β activation permits airway epithelial cell production of NF-κB-dependent genes involved in airway inflammation. However, since GSK-3β is constitutively active, it is unlikely that OVA treatment induced airway inflammation by increasing GSK-3β activation. Indeed, we found that OVA treatment increased the abundance of inactivated pGSK in the airway epithelium and inflammatory cells. OVA treatment also increased whole lung GSK-3β phosphorylation and decreased whole lung GSK-3β kinase activity. In any event, our data suggest that, based on its regulation of contractile protein expression, GSK-3β plays a unique role in ASM.

We used unbiased stereological morphometry to study the biochemical mechanisms underlying allergen-induced asthma. Similar stereological tools have been used previously, for example to assess ozone-induced cytotoxicity in tracheobronchial airways of the isolated perfused rat lung (29), differential proliferation of rat airway epithelial cells after keratinocyte growth factor administration (10), and ASM cell number and contractile protein expression in subjects with asthma (39). Confocal microscopy has been found ideally suited for the three-dimensional sampling of design-based stereology with the caveat that users must develop their own procedures (28) such as those discussed here using NIH ImageJ software.

In conclusion, OVA sensitization and challenge induces both ASM hypertrophy and hyperplasia in BALB/c mice. GSK-3β appears to be an important regulator of ASM cell size in this model. Future studies using stereological tools could provide insight into additional biochemical pathways involved in airway remodeling.

GRANTS

This work was supported by National Heart, Lung, and Blood Institute Grant HL-079339 (M. B. Hershenson).

Notes

The costs of publication of this article were defrayed in part by the payment of page charges. The article must therefore be hereby marked "*advertisement*" in accordance with 18 U.S.C. Section 1734 solely to indicate this fact.

REFERENCES

1. Antos CL, McKinsey TA, Frey N, Kutschke W, McAnally J, Shelton JM, Richardson JA, Hill JA, Olson EN. Activated glycogen synthase-3 beta suppresses cardiac hypertrophy in vivo. *Proc Natl Acad Sci USA* 99: 907–912, 2002. [PMCID: PMC117404] [PubMed: 11782539]

2. Armstrong DD, Esser KA. Wnt/β-catenin signaling activates growth-control genes during overload-induced skeletal muscle hypertrophy. *Am J Physiol Cell Physiol* 289: C853–C859, 2005. [PubMed: 15888552]

3. Badorff C, Ruetten H, Mueller S, Stahmer M, Gehring D, Jung F, Ihling C, Zeiher AM, Dimmeler S. Fas receptor signaling inhibits glycogen synthase kinase 3 beta and induces cardiac hypertrophy following pressure overload. *J Clin Invest* 109: 373–381, 2002. [PMCID: PMC150855] [PubMed: 11827997]

4. Bao Z, Lim S, Liao W, Lin Y, Thiemermann C, Leung BP, Wong WS. Glycogen synthase kinase-3beta inhibition attenuates asthma in mice. *Am J Respir Crit Care Med* 176: 431–438, 2007. [PubMed: 17556716]

5. Benayoun L, Druilhe A, Dombret MC, Aubier M, Pretolani M. Airway structural alterations selectively associated with severe asthma. *Am J Respir Crit Care Med* 167: 1360–1368, 2003. [PubMed: 12531777]

6. Cohen P, Frame S. The renaissance of GSK3. *Nat Rev Mol Cell Biol* 2: 769–776, 2001. [PubMed: 11584304]

7. Deng H, Dokshin GA, Lei J, Goldsmith AM, Bitar KN, Fingar DC, Hershenson MB, Bentley JK. Inhibition of glycogen synthase kinase-3β is sufficient for airway smooth muscle hypertrophy. *J Biol Chem* 283: 10198–10207, 2008. [PMCID: PMC2442285] [PubMed: 18252708]

8. Dorph-Petersen KA, Nyengaard JR, Gundersen HJ. Tissue shrinkage and unbiased stereological estimation of particle number and size. *J Microsc* 204: 232–246, 2001. [PubMed: 11903800]

9. Ebina M, Takahashi T, Chiba T, Motomiya M. Cellular hypertrophy and hyperplasia of airway smooth muscles underlying bronchial asthma. A 3-D morphometric study. *Am Rev Respir Dis* 148: 720–726, 1993. [PubMed: 8368645]

10. Fehrenbach H, Fehrenbach A, Pan T, Kasper M, Mason RJ. Keratinocyte growth factor-induced proliferation of rat airway epithelium is restricted to clara cells in vivo. *Eur Respir J* 20: 1185–1197, 2002. [PubMed: 12449173]

11. Gosens R, Dueck G, Rector E, Nunes RO, Gerthoffer WT, Unruh H, Zaagsma J, Meurs H, Halayko AJ. Cooperative regulation of GSK-3 by muscarinic and PDGF receptors is associated with airway myocyte proliferation. *Am J Physiol Lung Cell Mol Physiol* 293: L1348–L1358, 2007. [PubMed: 17873004]

12. Haq S, Choukroun G, Kang ZB, Ranu H, Matsui T, Rosenzweig A, Molkentin JD, Alessandrini A, Woodgett J, Hajjar R, Michael A, Force T. Glycogen synthase kinase-3beta is a negative regulator of cardiomyocyte hypertrophy. *J Cell Biol* 151: 117–130, 2000. [PMCID: PMC2189812] [PubMed: 11018058]

13. Haq S, Michael A, Andreucci M, Bhattacharya K, Dotto P, Walters B, Woodgett J, Kilter H, Force T. Stabilization of beta-catenin by a Wnt-independent mechanism regulates cardiomyocyte growth. *Proc Natl Acad Sci USA* 100: 4610–4615, 2003. [PMCID: PMC153603] [PubMed: 12668767]

14. Hardt SE, Tomita H, Katus HA, Sadoshima J. Phosphorylation of eukaryotic translation initiation factor 2Bε by glycogen synthase kinase-3β regulates β-adrenergic cardiac myocyte hypertrophy. *Circ Res* 94: 926–935, 2004. [PubMed: 15001529]

15. Henderson WR, Chiang GK, Tien YT, Chi EY. Reversal of allergen-induced airway remodeling by CysLt1 receptor blockade. *Am J Respir Crit Care Med* 173: 718–728, 2006. [PMCID: PMC2662952] [PubMed: 16387808]

16. Henderson WR, Tang LO, Chu SJ, Tsao SM, Chiang GK, Jones F, Jonas M, Pae C, Wang H, Chi EY. A role for cysteinyl leukotrienes in airway remodeling in a mouse asthma model. *Am J Respir Crit Care Med* 165: 108–116, 2002. [PubMed: 11779739]

17. Inoki K, Ouyang H, Zhu T, Lindvall C, Wang Y, Zhang X, Yang Q, Bennett C, Harada Y, Stankunas K, Wang CY, He X, MacDougald OA, You M, Williams BO, Guan KL. TSC2 integrates Wnt and energy signals via a coordinated phosphorylation by AMPK and GSK3 to regulate cell growth. *Cell* 126: 955–968, 2006. [PubMed: 16959574]

18. Leigh R, Ellis R, Wattie J, Southam DS, De Hoogh M, Gauldie J, O'Byrne PM, Inman MD. Dysfunction and remodeling of the mouse airway persist after resolution of acute allergen-induced airway inflammation. *Am J Respir Cell Mol Biol* 27: 526–535, 2002. [PubMed: 12397011]

19. McMillan SJ, Xanthou G, Lloyd CM. Manipulation of allergen-induced airway remodeling by treatment with anti-TGF-β antibody: effect on the Smad signaling pathway. *J Immunol* 174: 5774–5780, 2005. [PubMed: 15843580]

20. Moir LM, Leung SY, Eynott PR, McVicker CG, Ward JP, Chung KF, Hirst SJ. Repeated allergen inhalation induces phenotypic modulation of smooth muscle in bronchioles of sensitized rats. *Am J Physiol Lung Cell Mol Physiol* 284: L148–L159, 2003. [PubMed: 12388362]

21. Morisco C, Seta K, Hardt SE, Lee Y, Vatner SF, Sadoshima J. Glycogen synthase kinase 3beta regulates GATA4 in cardiac myocytes. *J Biol Chem* 276: 28586–28597, 2001. [PubMed: 11382772]

22. Morisco C, Zebrowski D, Condorelli G, Tsichlis P, Vatner SF, Sadoshima J. The Akt-glycogen synthase kinase 3beta pathway regulates transcription of atrial natriuretic factor induced by beta-adrenergic receptor stimulation in cardiac myocytes. *J Biol Chem* 275: 14466–14475, 2000. [PubMed: 10799529]

23. Mouton PR, Price DL, Walker LC. Empirical assessment of synapse numbers in primate neocortex. *J Neurosci Methods* 75: 119–126, 1997. [PubMed: 9288643]

24. Nath P, Leung SY, Williams A, Noble A, Chakravarty SD, Luedtke GR, Medicherla S, Higgins LS, Protter A, Chung KF. Importance of p38 mitogen-activated protein kinase pathway in allergic airway remodelling and bronchial hyperresponsiveness. *Eur J Pharmacol* 544: 160–167, 2006. [PubMed: 16843456]

25. Nunes RO, Schmidt M, Dueck G, Baarsma H, Halayko AJ, Kerstjens HA, Meurs H, Gosens R. GSK-3/β-catenin signaling axis in airway smooth muscle: Role in mitogenic signaling. *Am J Physiol Lung Cell Mol Physiol* 294: L1110–L1118, 2008. [PubMed: 18390827]

26. Panettieri RA, Murray RK, Eszterhas AJ, Bilgen G, Martin JG. Repeated allergen inhalations induce DNA synthesis in airway smooth muscle and epithelial cells in vivo. *Am J Physiol Lung Cell Mol Physiol* 274: L417–L424, 1998. [PubMed: 9530178]

27. Petersen MS, Petersen CC, Agger R, Hokland M, Gundersen HJ. A simple method for unbiased quantitation of adoptively transferred cells in solid tissues. *J Immunol Methods* 309: 173–181, 2006. [PubMed: 16413032]

28. Peterson DA Quantitative histology using confocal microscopy: implementation of unbiased stereology procedures. *Methods* 18: 493–507, 1999. [PubMed: 10491280]

29. Postlethwait EM, Joad JP, Hyde DM, Schelegle ES, Bric JM, Weir AJ, Putney LF, Wong VJ, Velsor LW, Plopper CG. Three-dimensional mapping of ozone-induced acute cytotoxicity in tracheobronchial airways of isolated perfused rat lung. *Am J Respir Cell Mol Biol* 22: 191–199, 2000. [PubMed: 10657940]

30. Rahmani M, Read JT, Carthy JM, McDonald PC, Wong BW, Esfandiarei M, Si X, Luo Z, Luo H, Rennie PS, McManus BM. Regulation of the versican promoter by the β-catenin-T-cell factor complex in vascular smooth muscle cells. *J Biol Chem* 280: 13019–13028, 2005. [PubMed: 15668231]

31. Rochat A, Fernandez A, Vandromme M, Molès JP, Bouschet T, Carnac G, Lamb NJ. Insulin and Wnt1 pathways cooperate to induce reserve cell activation in differentiation and myotube hypertrophy. *Mol Biol Cell* 15: 4544–4555, 2004. [PMCID: PMC519148] [PubMed: 15282335]

32. Salmon M, Walsh DA, Koto H, Barnes PJ, Chung KF. Repeated allergen exposure of sensitized Brown-Norway rats induces airway cell DNA synthesis and remodelling. *Eur Respir J* 14: 633–641, 1999. [PubMed: 10543287]

33. Steinbrecher KA, Wilson W 3rd, Cogswell PC, Baldwin AS. Glycogen synthase kinase 3β functions to specify gene-specific, NF-κB-dependent transcription. *Mol Cell Biol* 25: 8444–8455, 2005. [PMCID: PMC1265740] [PubMed: 16166627]

34. Sutherland C, Leighton IA, Cohen P. Inactivation of glycogen synthase kinase-3 beta by phosphorylation: new kinase connections in insulin and growth-factor signalling. *Biochem J* 296: 15–19, 1993. [PMCID: PMC1137648] [PubMed: 8250835]

35. Törmänen KR, Uller L, Persson CG, Erjefält JS. Allergen exposure of mouse airways evokes remodeling of both bronchi and large pulmonary vessels. *Am J Respir Crit Care Med* 171: 19–25, 2005. [PubMed: 15447945]

36. Vyas DR, Spangenburg EE, Abraha TW, Childs TE, Booth FW. GSK-3β negatively regulates skeletal myotube hypertrophy. *Am J Physiol Cell Physiol* 283: C545–C551, 2002. [PubMed: 12107064]

37. Welsh GI, Miller CM, Loughlin AJ, Price NT, Proud CG. Regulation of eukaryotic initiation factor eIF2B: glycogen synthase kinase-3 phosphorylates a conserved serine which undergoes dephosphorylation in response to insulin. *FEBS Lett* 421: 125–130, 1998. [PubMed: 9468292]

38. Wenzel SE, Schwartz LB, Langmack EL, Halliday JL, Trudeau JB, Gibbs RL, Chu HW. Evidence that severe asthma can be divided pathologically into two inflammatory subtypes with distinct physiologic and clinical characteristics. *Am J Respir Crit Care Med* 160: 1001–1008, 1999. [PubMed: 10471631]

39. Woodruff PG, Dolganov GM, Ferrando RE, Donnelly S, Hays SR, Solberg OD, Carter R, Wong HH, Cadbury PS, Fahy JV. Hyperplasia of smooth muscle in mild to moderate asthma without changes in cell size or gene expression. *Am J Respir Crit Care Med* 169: 1001–1006, 2004. [PubMed: 14726423]

Figures and Tables

Fig. 1.

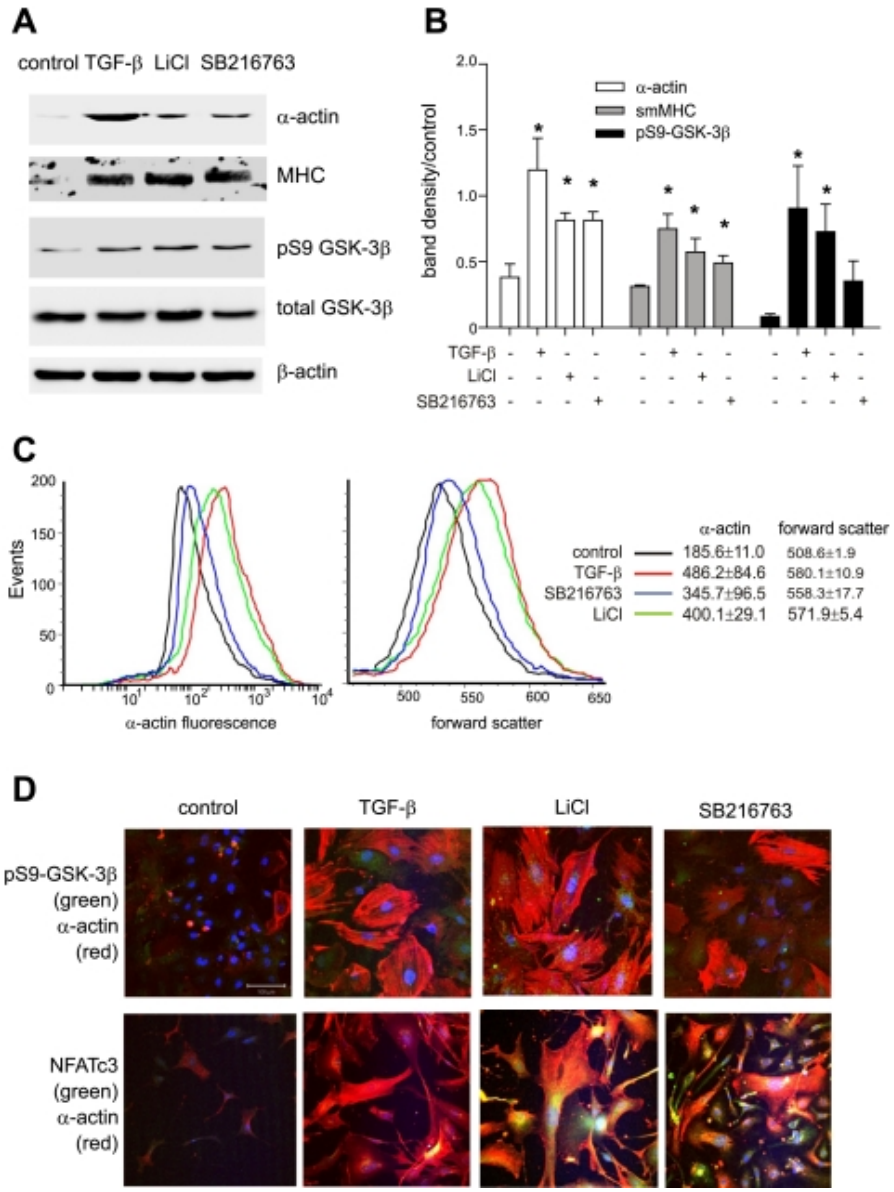

Glycogen synthase kinase-3β (GSK-3β) inhibition increases cell size and contractile protein synthesis in cultured murine airway smooth muscle (ASM) cells. *A*: mouse ASM cells from control animals were serum-deprived and treated with 10 ng/ml transforming growth factor (TGF)-β or the GSK-3β inhibitors 10 mM LiCl or 50 nM SB-216763. After 3 days of treatment, samples were processed for Western blots using antibodies to α-actin, myosin heavy chain (MHC), phospho-Ser^{9} GSK-3β (pS9 GSK-3β), total GSK-3β, and β-actin. *B*: group mean data for immunoblots as quantified by densitometry. Data are represented as fold increase over control. Data from 3 individual experiments are shown (*$P < 0.05$). *C*: mouse ASM cells were untreated (black line) or treated with 10 ng/ml TGF-β (red line), 50 nM SB-216763 (blue line), or 10 mM LiCl (green line). Cells were trypsinized, immunostained with anti-α-actin-FITC, and processed for flow cytometry. TGF-β, SB-216763, and LiCl each significantly increased cell size (as measured by forward scatter) and α-actin immunostaining (*$P <$ 0.05, 1-way ANOVA; $n = 3$). *D*: fluorescence confocal microscopy. Cells were treated with vehicle, TGF-β, LiCl, or SB-216763 immunostained with rabbit anti-pGSK (green channel, *top* 3 frames) or anti-NFATc3 (green channel, *bottom* 3 frames) and

anti-α-actin-Cy3 (red channel). Nuclei were counterstained with Hoechst 33342 (blue channel). Merged images are shown. In the cytoplasm, colocalization of pGSK or NFATc3 with α-actin is orange to yellow. Localization of pGSK or NFATc3 in the nucleus is pale blue (without α-actin) or white (with α-actin). Both TGF-β and GSK-3β inhibitors increased cell size, pGSK content, nuclear localization of NFAT, and α-actin expression. The white bar is 100 μm, and all images are to the same scale. sm, Smooth muscle.

Fig. 2.

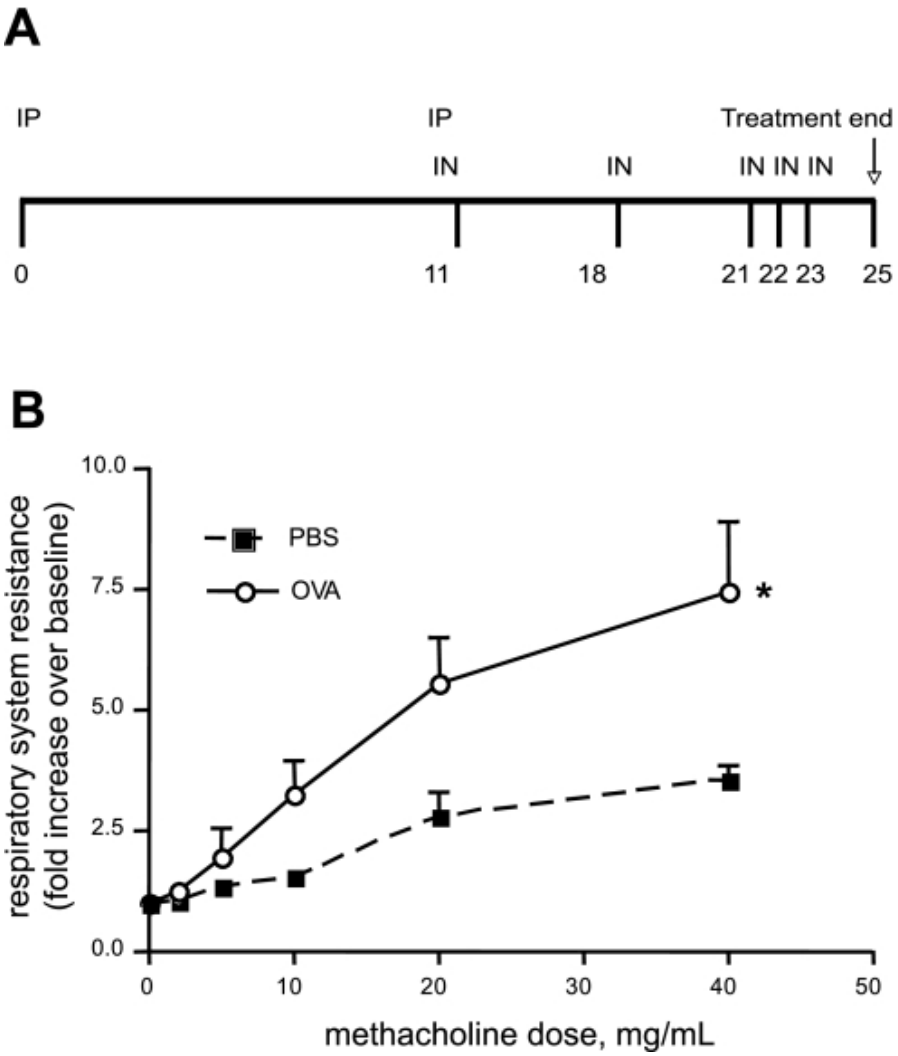

Ovalbumin (OVA) treatment increases cholinergic airways responsiveness in BALB/c mice. *A*: time course of OVA sensitization and challenge. On *day 0*, mice were injected intraperitoneally (IP) with 1 mg of a sterile, endotoxin-free solution of OVA emulsified in 25% (wt/vol, final) alum suspension or an equivalent amount of alum alone for the PBS control group. On *day 11*, mice were given a similar IP injection as well as an intranasal (IN) inoculation with 1 mg of OVA dissolved in 50 μl of PBS or PBS alone. Mice were allowed to recover and inoculated again with IN PBS or OVA on *days 18*, *21*, *22*, and *23*. Mice were studied on *day 25*. *B*: PBS-treated (▪) or OVA-treated (○) mice were examined for airways resistance using a positive displacement respirometer and increasing doses of nebulized methacholine in PBS ($n = 3$, means ± SE; $^*P < 0.05$, 2-way ANOVA).

Fig. 3.

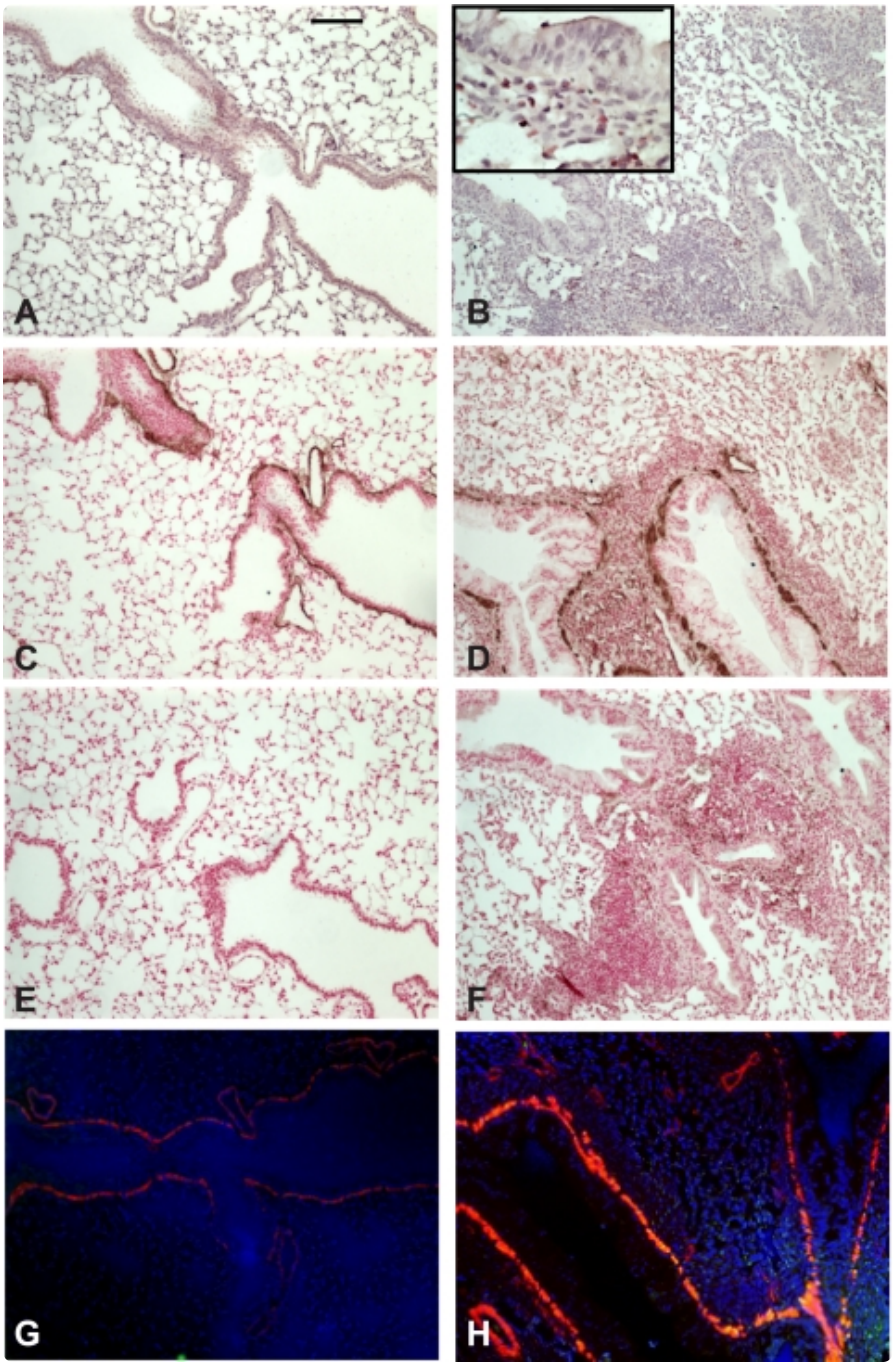

OVA treatment increases airway inflammation and ASM α-actin immunostaining. *A* and *B*: hematoxylin and eosin (H&E)-stained lung sections from PBS- and OVA-treated mice. *Inset* shows eosinophilic inflammation. *C*–*F*: lung sections were immunostained with anti-α-actin (*C* and *D*) or mouse IgG (*E* and *F*) and peroxidase-conjugated anti-mouse IgG and subsequently developed with diaminobenzidine and $NiCl_2$. Sections were counterstained with nuclear fast red. *G* and *H*: immunofluorescence staining of PBS- and OVA-treated mouse lungs using an anti-α-actin Cy3 conjugate (red) and rabbit anti-pGSK with goat anti-rabbit IgG-Alexa 488 secondary (green channel) antibodies. Nuclei were stained with Hoechst 33342 (blue). OVA-treated mice (*B*, *D*, *F*, and *H*) showed increased airway inflammation and α-actin immunostaining (*D*). Magnification is ×200, and black bars represent 100 μm.

Fig. 4.

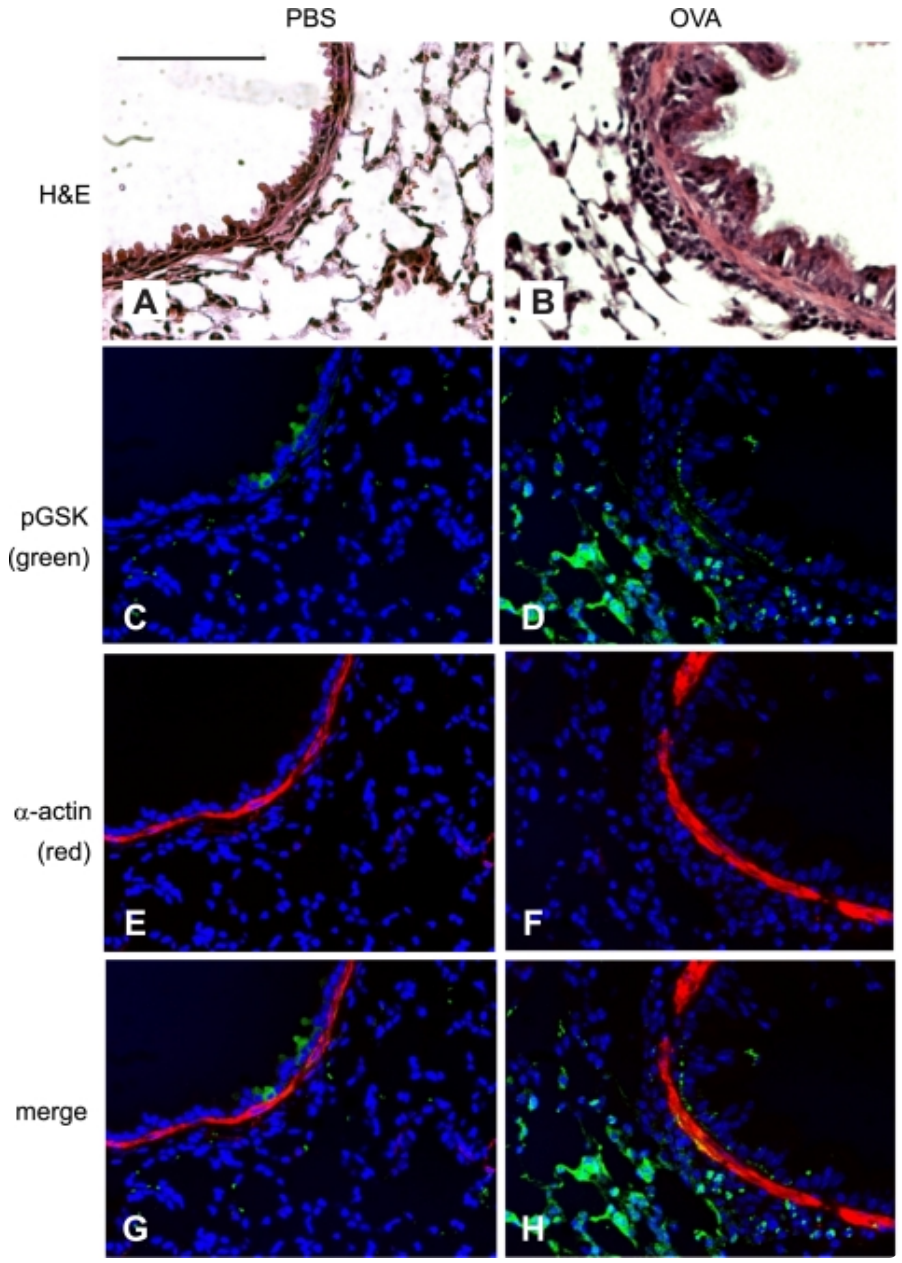

OVA treatment increases phospho-Ser[9] GSK-3β (pGSK) immunostaining in the airway epithelium and ASM. *A* and *B*: H&E-stained lung sections from PBS- and OVA-treated mice. *C*–*F*: lung sections were immunostained with anti-phospho-GSK-3β (green, *C* and *D*) or anti-α-actin Cy3 conjugate (red, *E* and *F*). Nuclei were stained with Hoechst 33342 (blue, *C*–*H*). Images were merged (*G* and *H*) to show colocalization of phospho-GSK-3β and α-actin. Colocalization varies in intensity from orange (relatively low pGSK) to yellow (higher pGSK). OVA-treated mice (*B*, *D*, *F*, and *H*) showed increased airway inflammation (*B*), phospho-GSK-3β (*D*), α-actin (*F*), and colocalization of phospho-GSK-3β and α-actin (*H*). Magnification is ×320, black bars represent 50 μm, and all panels are to the same scale.

Fig. 5.

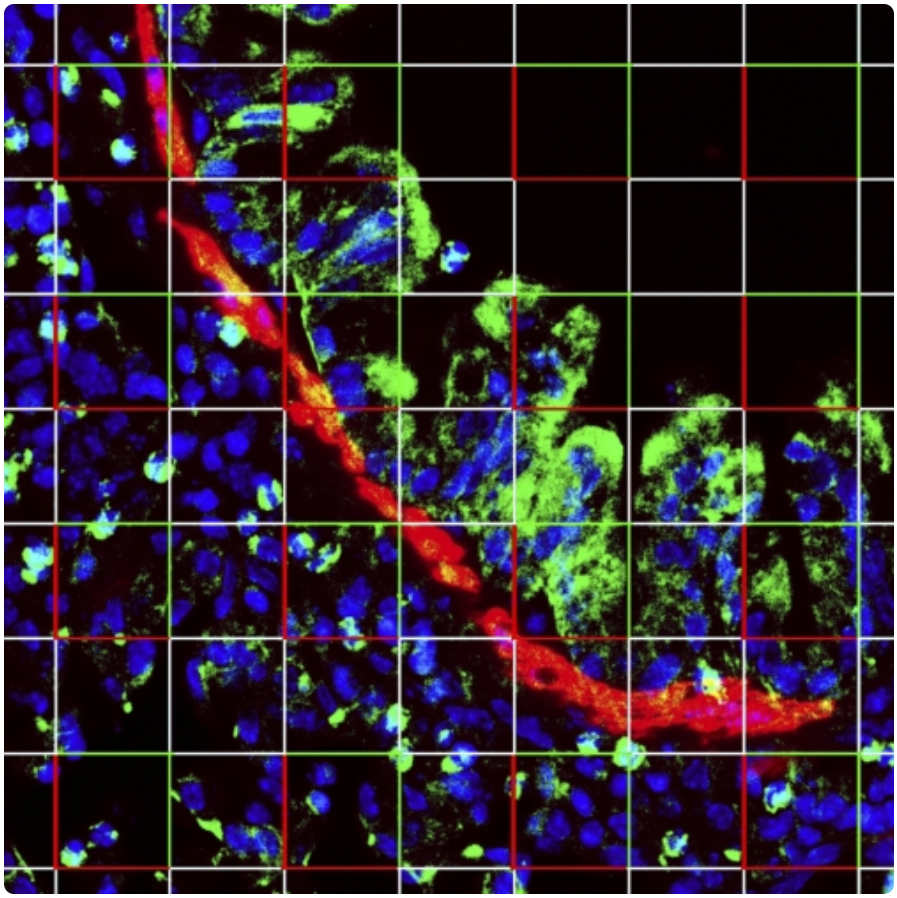

OVA treatment increases the number of pGSK (+) ASM. Nuclear counts of α-actin- and pGSK-staining cells were assessed by stereological analyses using an optical disector probe. Nuclei were visualized with Hoechst 33342 (blue), pGSK immunoreactivity (green), and α-actin (red). Colocalization of pGSK and α-actin appears yellow-orange. Using NIH ImageJ, a grid was overlaid on an entire 30-μm-thick *z*-series stack, as in this figure, and nuclei from α-actin-positive cells were counted as they came into focus through the stack using the optical disector counting rules. Nuclei touching the bright red corners of the indicated squares were not counted, whereas nuclei touching the green borders were allowed. Consistent with stereological counting rules, no immediately adjacent squares were counted. Magnification, ×400.

Fig. 6.

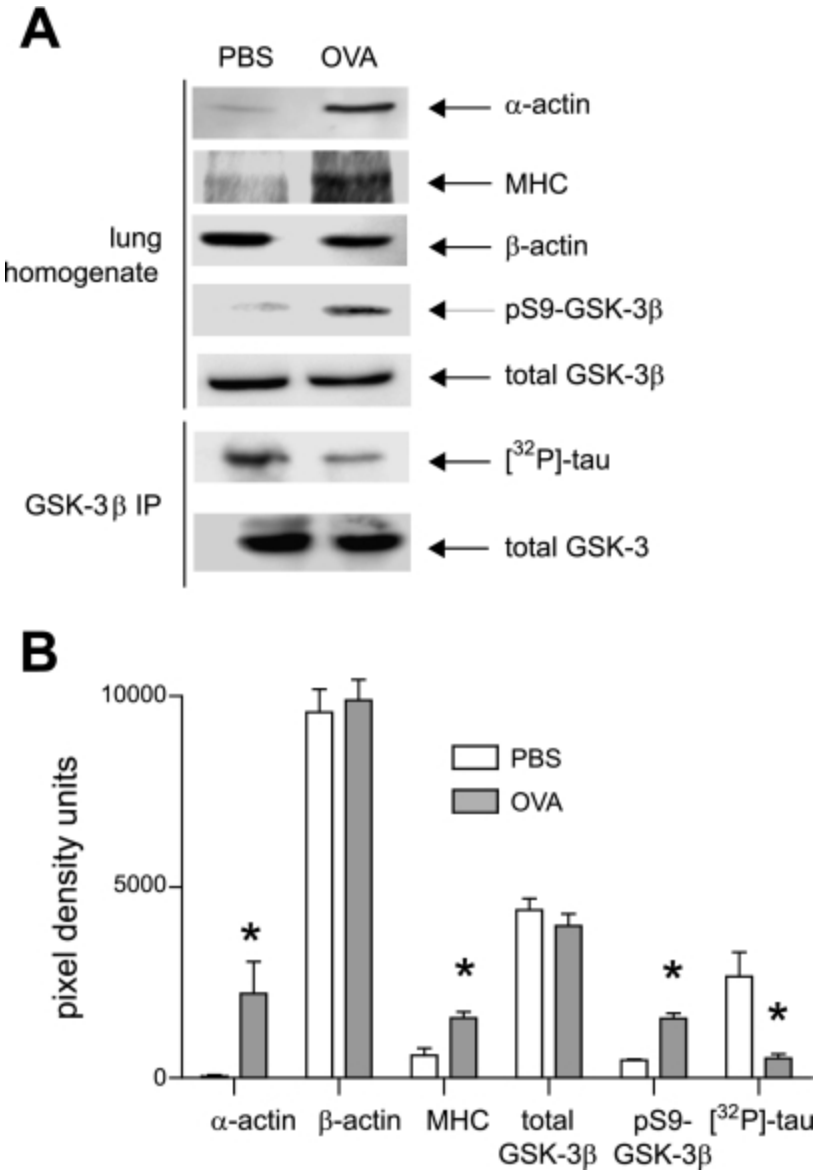

OVA treatment increases whole lung pGSK content and decreases whole lung GSK-3β kinase activity. *A*: lungs from PBS or OVA-sensitized mice were homogenized, and 20 μg of protein was assessed by immunoblotting for α-actin, β-actin, phospho-Ser[9], and total GSK-3β. For MHC, 50 μg of protein was processed. In addition, GSK-3β was immunoprecipitated from 1 mg of soluble lung protein, and GSK-3β activity was assessed using recombinant tau as a substrate. Changes in phosphorylation were not due to a difference in the GSK-3β content of immunoprecipitates. *B*: group mean data for pixel densitometry scans using NIH ImageJ software ($n = 3$; $^*P < 0.05$, ANOVA).

Table 1.

Ovalbumin (OVA) sensitization increases the total volume of airway smooth muscle (ASM) as well as the number and size of individual ASM cells. ASM was identified by α-actin immunostaining

Treatment	PBS	OVA
Lung volume, ml	0.99±0.02	1.25±0.1*
ASM Vv	0.006±0.0003	0.014±0.001†
ASM volume, ml per lung	0.005±0.001	0.017±0.004†
ASM Nv	$7.09\times10^6\pm4.63\times10^5$	$10.9\times10^6\pm7.61\times10^5$†
ASM cells per lung	$6.03\times10^6\pm6.27\times10^5$	$12.8\times10^6\pm7.31\times10^5$‡
ASM Vv/Nv, μm^3	824±76	1,310±183†

Values are means ± SE; $n = 6$ for each condition; different from PBS group,
*$P < 0.05$,
†$P < 0.002$, and
‡$P < 0.001$, unpaired *t*-test. Vv, ASM fractional unit volume or volume density; Nv, ASM number per unit volume.

Table 2.

OVA treatment increases the volume and number of pGSK (+) ASM

Treatment	PBS	OVA
pGSK (+) ASM Vv	0.001±0.0001	0.012±0.0008†
pGSK (−) ASM Vv	0.004±0.0005	0.003±0.0007
pGSK (+) ASM lung volume, ml	0.001±0.0002	0.015±0.001†
pGSK (+) ASM Nv	$1.88\times10^6\pm1.52\times10^5$	$9.58\times10^6\pm4.19\times10^5$‡
pGSK (+) ASM cells per lung	$1.59\times10^6\pm1.84\times105$	$11.2\times10^6\pm3.56\times10^5$†
pGSK (−) ASM Nv	$5.71\times10^6\pm6.61\times10^5$	$3.81\times10^6\pm8.29\times10^5$*
pGSK (+) ASM Vv/Nv, μm^3	768±109	1230±193‡
pGSK (−) ASM Vv/Nv, μm^3	802±96	722±211

Values are means ± SE; $n = 6$ for each condition; different from PBS group,
*$P < 0.05$,
†$P < 0.002$,
‡$P < 0.001$, unpaired *t*-test. pGSK, phospho-Ser^9 glycogen synthase kinase-3β.